

# Major Loci on Chromosomes 8q and 3q Control Interferon $\gamma$ Production Triggered by Bacillus Calmette-Guerin and 6-kDa Early Secretory Antigen Target, Respectively, in Various Populations

Fabienne Jabot-Hanin,<sup>1,2</sup> Aurélie Cobat,<sup>1,2</sup> Jacqueline Feinberg,<sup>1,2</sup> Ghislain Grange,<sup>1,2</sup> Natascha Remus,<sup>1,2</sup> Christine Poirier,<sup>5</sup> Anne Boland-Auge,<sup>6</sup> Céline Besse,<sup>6</sup> Jacinta Bustamante,<sup>1,2</sup> Stéphanie Boisson-Dupuis,<sup>1,2,7</sup> Jean-Laurent Casanova,<sup>1,2,3,7,8</sup> Erwin Schurr,<sup>9,10,11</sup> Alexandre Alcaïs,<sup>1,2,7</sup> Eileen G. Hoal,<sup>12</sup> Christophe Delacourt,<sup>4</sup> and Laurent Abel<sup>1,2,7</sup>

<sup>1</sup>Laboratory of Human Genetics of Infectious Diseases, Necker Branch, INSERM U1163, <sup>2</sup>Paris Descartes University, Sorbonne Paris Cité, Imagine Institute, <sup>3</sup>Pediatric Hematology-Immunology Unit and <sup>4</sup>Pediatric Pneumology Unit, Necker Hospital for Sick Children, AP-HP, Paris; <sup>5</sup>Centre de Lutte Anti-Tuberculeuse, Centre Hospitalier Intercommunal de Créteil, and <sup>6</sup>Centre National de Génotypage, Institut de Génétique, CEA, Evry, France; <sup>7</sup>St Giles Laboratory of Human Genetics of Infectious Diseases, Rockefeller Branch, Rockefeller University, and <sup>8</sup>Howard Hughes Medical Institute, New York, New York; <sup>9</sup>McGill International TB Centre, <sup>10</sup>Department of Human Genetics, and <sup>11</sup>Department of Medicine, McGill University, Montreal, Canada; and <sup>12</sup>Division of Molecular Biology and Human Genetics, MRC Centre for Molecular and Cellular Biology and DST/NRF Centre of Excellence for Biomedical TB Research, Faculty of Health Sciences, Stellenbosch University, Tygerberg, South Africa

**Background.** Interferon  $\gamma$  (IFN- $\gamma$ ) release assays (IGRAs) provide an in vitro measurement of antimycobacterial immunity that is widely used as a test for *Mycobacterium tuberculosis* infection. IGRA outcomes are highly heritable in various populations, but the nature of the involved genetic factors remains unknown.

**Methods.** We conducted a genome-wide linkage analysis of IGRA phenotypes in families from a tuberculosis household contact study in France and a replication study in families from South Africa to confirm the loci identified.

**Results.** We identified a major locus on chromosome 8q controlling IFN- $\gamma$  production in response to stimulation with live bacillus Calmette-Guerin (BCG; LOD score, 3.81;  $P = 1.40 \times 10^{-5}$ ). We also detected a second locus, on chromosome 3q, that controlled IFN- $\gamma$  levels in response to stimulation with 6-kDa early secretory antigen target, when accounting for the IFN- $\gamma$  production shared with that induced by BCG (LOD score, 3.72;  $P = 1.8 \times 10^{-5}$ ). Both loci were replicated in South African families, where tuberculosis is hyperendemic. These loci differ from those previously identified as controlling the response to the tuberculin skin test (*TST1* and *TST2*) and the production of TNF- $\alpha$  (*TNFI*).

**Conclusions.** The identification of 2 new linkage signals in populations of various ethnic origins living in different *M. tuberculosis* exposure settings provides new clues about the genetic control of human antimycobacterial immunity.

**Keywords.** tuberculosis; genetic linkage analysis; interferon gamma release assays; mycobacteria; genetic control.

Tuberculosis remains a major public health problem, with *Mycobacterium tuberculosis* currently infecting an estimated one third of the world's population and approximately 9 million new cases of and 1.5 million deaths due to tuberculosis in 2013 [1, 2]. *M. tuberculosis* bacilli are transmitted by inhalation of aerosolized droplets generated by the coughing of patients with infectious tuberculosis. There is no direct proof of latent *M. tuberculosis* infection (hereafter, "latent infection") in exposed individuals, and the infection phenotype is inferred indirectly from quantitative measurements of antimycobacterial

immunity, attesting to previous exposure to *M. tuberculosis* [3]. The tuberculin skin test (TST) is the most widely used method to test for latent infection [4], although it suffers from a lack of specificity, partly due to cross-reactions with bacillus Calmette-Guerin (BCG) and, to a lesser extent, environmental mycobacteria. Additional assays to detect latent infection, based on in vitro evaluations of T-cell antimycobacterial immunity, have been developed over the last 15 years [5]. They measure the secretion of interferon  $\gamma$  (IFN- $\gamma$ ) by circulating leukocytes in response to *M. tuberculosis* antigens, such as 6-kDa early secretory antigen target (ESAT-6) and 10-kDa culture filtrate protein [6]. ESAT-6 is encoded neither by the BCG strain used for vaccination nor by most environmental mycobacteria [7]. These IFN- $\gamma$  release assays (IGRAs) yield results that are not fully concordant with TST findings, but they provide complementary information about infection status [8, 9].

Based on TST and IGRA results, an estimated 10%–20% of subjects do not become infected with *M. tuberculosis* despite sustained exposure and, hence, never develop disease [3, 10]. In addition, most infected subjects develop latent infection

Received 9 October 2015; accepted 11 December 2015; published online 21 December 2015.

Correspondence: L. Abel, Human Genetics of Infectious Diseases, Institut Imagine, 24 Bd du Montparnasse, 75015 Paris, France (laurent.abel@inserm.fr).

The Journal of Infectious Diseases® 2016;213:1173–9

© The Author 2015. Published by Oxford University Press for the Infectious Diseases Society of America. This is an Open Access article distributed under the terms of the Creative Commons Attribution-NonCommercial-NoDerivs licence (<http://creativecommons.org/licenses/by-nc-nd/4.0/>), which permits non-commercial reproduction and distribution of the work, in any medium, provided the original work is not altered or transformed in any way, and that the work is properly cited. For commercial re-use, contact [journals.permissions@oup.com](mailto:journals.permissions@oup.com). DOI: 10.1093/infdis/jiv757

without ever developing clinical tuberculosis [2, 3, 10, 11]. There is accumulating evidence that human genetic factors play an important role in the development of clinical tuberculosis [3, 10, 12], particularly with the identification of single-gene inborn errors of immunity predisposing to at least some cases of severe childhood tuberculosis [13]. Several studies focusing on TST reactivity have also provided evidence for the role of human genetic factors in different steps of the latent infection process [14–16]. In particular, a linkage study in families from South Africa mapped 2 major loci controlling TST positivity per se (*TST1* on 11p14) and the intensity of TST reactivity (*TST2* on 5p15) [17]. The *TST1* locus was recently replicated in French families of various ethnic origins [18]. The genetic factors influencing IGRA phenotypes have been less thoroughly studied. The heritability of IFN- $\gamma$  secretion has been estimated to be about 43% following BCG stimulation and 58% following ESAT-6 stimulation in South Africa [19] and to be 17%–48% following stimulation with *M. tuberculosis* antigens, including ESAT-6, in Uganda, depending on the TST status of those tested [20, 21]. In this study, we conducted a genome-wide linkage analysis (GWLA) of several phenotypes of IFN- $\gamma$  production in response to mycobacterial stimulation, initially in families from household tuberculosis contacts in a suburb of Paris, France, and then in families from South Africa.

## MATERIALS AND METHODS

### Subjects and Families

A prospective study of household tuberculosis contacts was conducted in Val-de-Marne, in the suburbs of Paris, as previously described [22]. Val-de-Marne is an area of low tuberculosis endemicity with an annual tuberculosis incidence of 22.1 cases per 100 000 at the time of the study, compared with an overall incidence of 8.8 cases per 100 000 in France. From April 2004 to January 2009, household contacts exposed to a patient with culture-confirmed pulmonary tuberculosis were enrolled in the context of a general screening procedure, as detailed in the [Supplementary Methods](#). This study was approved by the French Consultative Committee for Protecting Persons in Biomedical Research of Henri Mondor Hospital (Créteil, France). Written informed consent was obtained from all study participants and from parents of the enrolled minors/children.

As a replication cohort, we used 450 people from 135 nuclear families from Ravensmead and Uitsig, a suburban of Cape Town, South Africa, where tuberculosis is hyperendemic [23]. This sample had previously been used to map the *TST1* and *TST2* loci [17] and to study the heritability of antimycobacterial immunity [19].

### Measurement of IFN- $\gamma$ Production

For the Val-de-Marne sample, blood samples were collected from each individual, and peripheral blood mononuclear cells

(PBMCs) were isolated and activated with ESAT-6, purified protein derivative (PPD), live BCG, and phytohemagglutinin (PHA), as described in the [Supplementary Methods](#). For the Cape Town sample, IGRAs were performed in quadruplicate on whole-blood specimens with BCG, PPD, ESAT-6, and PHA stimulations, as previously described [8]. IFN- $\gamma$  levels were measured on days 3 and 7 after stimulation, but, for the sake of consistency with the primary cohort, we confined the analysis to the measurements made on day 3.

### Phenotypes and Covariates of Interest

Three phenotypes were studied: IFN- $\gamma$  production after stimulation with BCG, PPD, and ESAT-6. The distributions of IFN- $\gamma$  production after the various stimulations were strongly skewed to the left and were therefore subjected to classical log transformation. After this transformation, the nonstimulated control value was subtracted from the stimulated values. These transformed phenotypes were then adjusted by linear regression for risk factors selected from those recorded during recruitment [22]. The selected covariates were chosen on the basis of a significant association with at least one of the phenotypes studied in univariate analysis and to give the best fit in terms of the Akaike information criterion (AIC) in the final multivariate model. These adjusted phenotypes are referred to here as IFN $\gamma$ -BCG, IFN $\gamma$ -ESAT6, and IFN $\gamma$ -PPD. The distribution of IFN- $\gamma$  production before and after adjustment is shown in [Supplementary Figure 1](#). We also studied a fourth phenotype corresponding to IFN $\gamma$ -ESAT6 adjusted for IFN $\gamma$ -BCG, to isolate a more specific response to the ESAT-6 antigen in terms of IFN- $\gamma$  production, taking into account the effect shared between BCG and ESAT-6 stimulation. This phenotype is denoted IFN $\gamma$ -ESAT6<sub>BCG</sub>.

Relevant covariates for this analysis are detailed in the [Supplementary Methods](#) and [Supplementary Table 1](#). These covariates include the annual incidence of tuberculosis in the country of birth; the estimated exposure to the index case; the infectivity of the index case; the presence or absence of complementary health insurance coverage, for use as a marker of socioeconomic status; age; and a binary indicator of the time between TST administration and blood sampling. In the South African cohort, we performed multivariate linear regression analyses in which we used the geometric mean value of the 4 measurements of IFN- $\gamma$  production for the different types of stimulation, subtracted the logarithm of the value obtained in the absence of stimulation, and adjusted the resulting values for sex, age, and previous clinical tuberculosis, as previously described [19]. The IFN $\gamma$ -ESAT6 phenotype in the South African cohort was also adjusted for IFN $\gamma$ -BCG phenotype.

### Genetic Analysis

For the French sample, we used the Illumina linkage V panel to genotype children and their parents for the GWLA. Single-nucleotide polymorphisms (SNPs) with a call rate of <90%

were removed from the analysis, resulting in the use of 5376 autosomal informative SNPs for GWLA. The South African sample was genotyped with the Illumina linkage IVb panel, and, after quality control, 5657 autosomal SNPs were retained for linkage analyses [17]. Model-free GWLA of the adjusted IFN- $\gamma$  production phenotypes was performed with the new maximum-likelihood binomial (MLB) method for quantitative traits (nMLB-QTL v.3.0) [24, 25]. The MLB approach considers the sibship as a whole and makes no assumptions about the distribution of the phenotype. The results of the linkage test can be expressed as a classical LOD score [24, 25]. We used LOD scores of 3.6 and 2.2 as genome-wide significant and suggestive thresholds, respectively [26]. A LOD score of 0.5875 (corresponding to a *P* value of .05) was used as the replication threshold, as previously suggested [27].

To investigate the population structure of our cohort, we performed a principal component analysis (PCA) on 5350 markers of the Illumina linkage IVb panel common between our sample and the 1000 Genomes Project multiethnic reference panel (Phase I interim release, 2011), using the EIGENSTRAT method [28]. Data only for individuals involved in the 1000 Genomes Project were used for computation of the principal components, and data for the individuals from Val-de-Marne were projected one by one onto the eigenvectors with the smartpca package of EIGENSOFT [28].

## RESULTS

A flow chart describing the selection of subjects for this study is presented in [Supplementary Figure 2](#). Analyses of the covariates influencing the phenotypes of interest in the French sample were performed on 528 household tuberculosis contacts, of whom 268 were women and 260 were men from 143 pedigrees. Univariate and multivariate analyses ([Supplementary Table 1](#)) showed that higher levels of IFN- $\gamma$  production were associated with a higher incidence of tuberculosis in the country of birth, a longer duration of exposure to the index case, a higher infectivity of the index case (this effect being restricted to young individuals for the IFN $\gamma$ -BCG and IFN $\gamma$ -PPD phenotypes), and an absence of complementary health insurance coverage. IFN- $\gamma$  production increased significantly with age for the IFN $\gamma$ -ESAT6 and IFN $\gamma$ -PPD phenotypes but not for the IFN $\gamma$ -BCG phenotype, probably because of the high rate of BCG vaccination. The IFN- $\gamma$  production phenotypes were adjusted for the relevant covariates ([Supplementary Table 1](#)) for further analyses. After adjustment, a strong correlation was found ( $r = 0.78$ ) between IFN $\gamma$ -BCG and IFN $\gamma$ -PPD, and a weaker correlation ( $r = 0.53$ ) was detected between IFN $\gamma$ -BCG and IFN $\gamma$ -ESAT6 ([Table 1](#)). As described in “Methods” section, IFN $\gamma$ -ESAT6 was also adjusted for IFN $\gamma$ -BCG and for the covariates shown in [Supplementary Table 1](#) (IFN $\gamma$ -ESAT6<sub>BCG</sub>).

GWLA was performed on 97 informative families, each including 2–6 offspring with available phenotypes and containing 240 siblings in total. Based on the 2 first principal components of

**Table 1. Spearman Correlation Coefficients for the Relationships Between the 4 Phenotypes of Interferon  $\gamma$  Production Used for Genome-Wide Linkage Analysis and Tuberculin Skin Testing (TST) in the Val-de-Marne Sample**

| Phenotype                          | IFN $\gamma$ -BCG | IFN $\gamma$ -PPD | IFN $\gamma$ -ESAT6 | IFN $\gamma$ -ESAT6 <sub>BCG</sub> | TST <sup>a</sup> |
|------------------------------------|-------------------|-------------------|---------------------|------------------------------------|------------------|
| IFN $\gamma$ -BCG                  | 1                 | 0.78              | 0.53                | 0.02                               | 0.09             |
| IFN $\gamma$ -PPD                  | 0.78              | 1                 | 0.61                | 0.25                               | 0.2              |
| IFN $\gamma$ -ESAT6                | 0.53              | 0.61              | 1                   | 0.86                               | 0.07             |
| IFN $\gamma$ -ESAT6 <sub>BCG</sub> | 0.02              | 0.25              | 0.86                | 1                                  | 0.02             |
| TST                                | 0.09              | 0.2               | 0.07                | 0.02                               | 1                |

Phenotypes are described in “Materials and Methods” section.

Abbreviations: BCG, bacillus Calmette-Guerin; ESAT, early secretory antigen target; IFN $\gamma$ , interferon  $\gamma$ ; PPD, purified protein derivative.

<sup>a</sup> Adjusted as described by Cobat et al [18].

the PCA, the 97 studied families could be divided into 49 from Europe or North Africa, 36 from sub-Saharan Africa (AFR), and 12 from other origins, including Asia ([Supplementary Figure 3](#)). Information content (IC) was high across all autosomes, with a mean genome-wide information value of 87.6% (range, 69%–94%). The results for the GWLA of the IFN $\gamma$ -BCG phenotype are shown in [Figure 1A](#). A significant linkage signal was observed on chromosome region 8q21.13, with a LOD score of 3.80 ( $P = 1.4 \times 10^{-5}$ ), at 82.7 Mb (IC = 86%). In addition, we also found a suggestive linkage signal on chromosome 5q35 (LOD score = 2.48, IC = 86.4%), and seven weaker linkage peaks with LOD scores of >1.17 (ie,  $P < .01$ ; [Supplementary Table 2](#)). The most significant GWLA peak observed for the IFN $\gamma$ -PPD phenotype was also on chromosome region 8q21.13, with a LOD score of 3.03 (IC = 89.9%), at 79 Mb ([Supplementary Figure 4](#)), consistent with the strong correlation between IFN $\gamma$ -PPD and IFN $\gamma$ -BCG. Among the 97 families used for the analysis, 39% of families from Europe or North Africa, 36% from sub-Saharan Africa, and 41% from other origins were contributing to the significant linkage signal observed for the IFN $\gamma$ -BCG phenotype (ie, LOD score >0.1 in the linkage region). This result shows that the observed linkage signal was supported by families from the different ethnic backgrounds present in our sample.

We then performed a replication study for the 2 chromosomal regions identified, 8q21 and 5q35, in the South African sample, with the adjusted IFN $\gamma$ -BCG phenotype. The suggestive 5q35 signal was not significant in the South African sample (maximal LOD score = 0.14), but we were able to replicate linkage to the 8q21 region with a LOD score of 0.98 ( $P = .016$ ) at 70 Mb ([Figure 1B](#)). No other significant linkage signal for IFN $\gamma$ -BCG phenotype was found in the Cape Town sample (the highest LOD score reached 2.06 at 83 Mb on chromosome 16). Additional support for linkage to the IFN $\gamma$ -BCG phenotype was provided by summing the LOD scores of the 2 samples with a LOD score of 4.50 at 69.7 Mb ([Figure 1B](#)). Given the variability of estimates of location in linkage studies of complex traits [29] and the slight differences in phenotype definition between

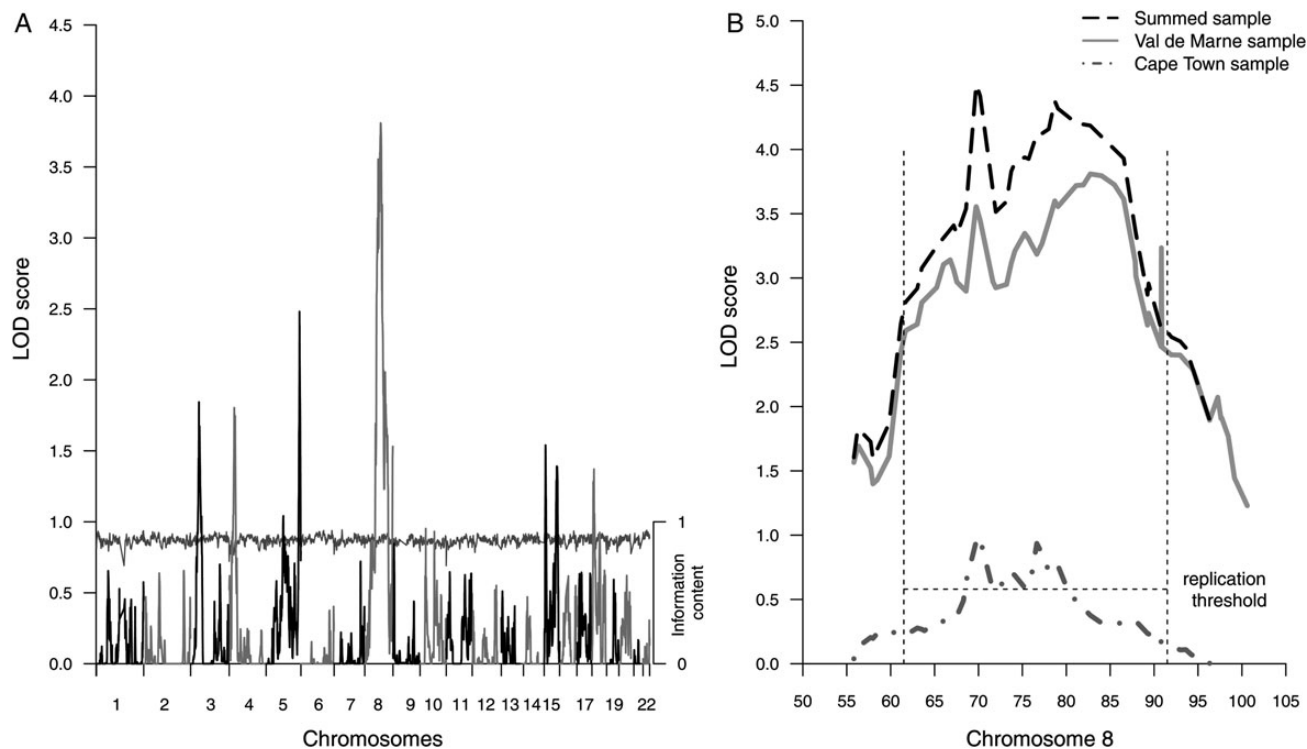


**Figure 1.** Model-free linkage analysis of the IFN $\gamma$ -BCG phenotype described in “Materials and Methods” section. *A*, Results of genome-wide analysis for the Val de Marne sample, showing multipoint LOD scores (left  $y$ -axis) and information content (horizontal line; right  $y$ -axis) for the 22 autosomes ( $x$ -axis). *B*, Expanded view of the linked chromosome 8 region from 55 to 100 Mb ( $x$ -axis); the multipoint LOD score is shown on the  $y$ -axis for the Val-de-Marne sample (solid gray line), the Cape Town sample (double-dashed gray line), and the summed samples (black long-dash line). The horizontal dotted line indicates the significance threshold for replication, and the 2 vertical dotted lines delimit the confidence interval of the linked locus.

our samples, it seems reasonable to consider a rather large confidence interval for the locus influencing the IFN $\gamma$ -BCG phenotype. Based on the curve of the summed LOD scores, we considered that this interval was between 61 and 91.5 Mb on chromosome 8 (Figure 1*B*). This region contains 108 known genes (Supplementary Table 3), including the gene (*IL7*) that encodes interleukin 7, which is required for the development and homeostasis of human T lymphocytes [30, 31]. Another interesting gene in this region is *LY96*, which encodes a protein that cooperates with Toll-like receptor 2 (TLR2) in the response to cell wall components from gram-positive and gram-negative bacteria [32]. Finally, this region borders the 8q12-13 region (55.1–61.2 Mb) that was previously reported to be linked to pulmonary tuberculosis in Morocco [33] and including the *TOX* gene (at 59.7–60 Mb), variants of which are associated with early onset pulmonary tuberculosis [34]. Overall, the present linkage analysis results highlight a major locus in chromosomal region 8q12-8q22 controlling the amount of IFN- $\gamma$  produced in response to BCG.

The GWLA of the IFN $\gamma$ -ESAT6 phenotype identified no significant linkage signal, with a maximum LOD score of 2.19 ( $P = 7.4 \times 10^{-4}$ ) at 122 Mb on chromosome 3 (Supplementary Figure 5). However, when IFN $\gamma$ -ESAT6 was adjusted for the

IFN $\gamma$ -BCG phenotype, the linkage signal on chromosome 3q13-22 became significant, with a LOD score of 3.72 ( $P = 1.8 \times 10^{-5}$ ) at 122.3 Mb (IC = 90.9%; Figure 2). No other suggestive linkage peaks were found with the IFN $\gamma$ -ESAT6<sub>BCG</sub> phenotype, and there were 4 weaker linkage signals with  $P$  values of  $<.01$  (Supplementary Table 3). Among the 97 families used for the analysis, 39% from Europe or North Africa, 25% from sub-Saharan Africa, and 41% from other origins were contributing to the linkage signal observed for the IFN $\gamma$ -ESAT6<sub>BCG</sub> phenotype, indicating that this linkage signal was also resulting from families of different ethnic origins. The chromosome 3q signal obtained with the IFN $\gamma$ -ESAT6<sub>BCG</sub> phenotype was replicated in the South African sample, with LOD scores of 0.78 ( $P = .028$ ) at 125.7 Mb and 1.31 ( $P = .007$ ) at 138.7 Mb. No other significant linkage signal for IFN $\gamma$ -ESAT6<sub>BCG</sub> phenotype was found in the Cape Town sample (the highest LOD score reached 1.8 at 4.5 Mb on chromosome 19). When the LOD scores for the 2 samples were summed, the maximum LOD score was 4.16 at 123.5 Mb. For the reasons given above, we considered that the linked region extended from 115 to 139 Mb (Figure 2).

The 180 known genes in this region (Supplementary Table 4) include *GATA2*, which encodes a transcription factor involved in the homeostasis of hematopoietic stem cells, haploinsufficiency

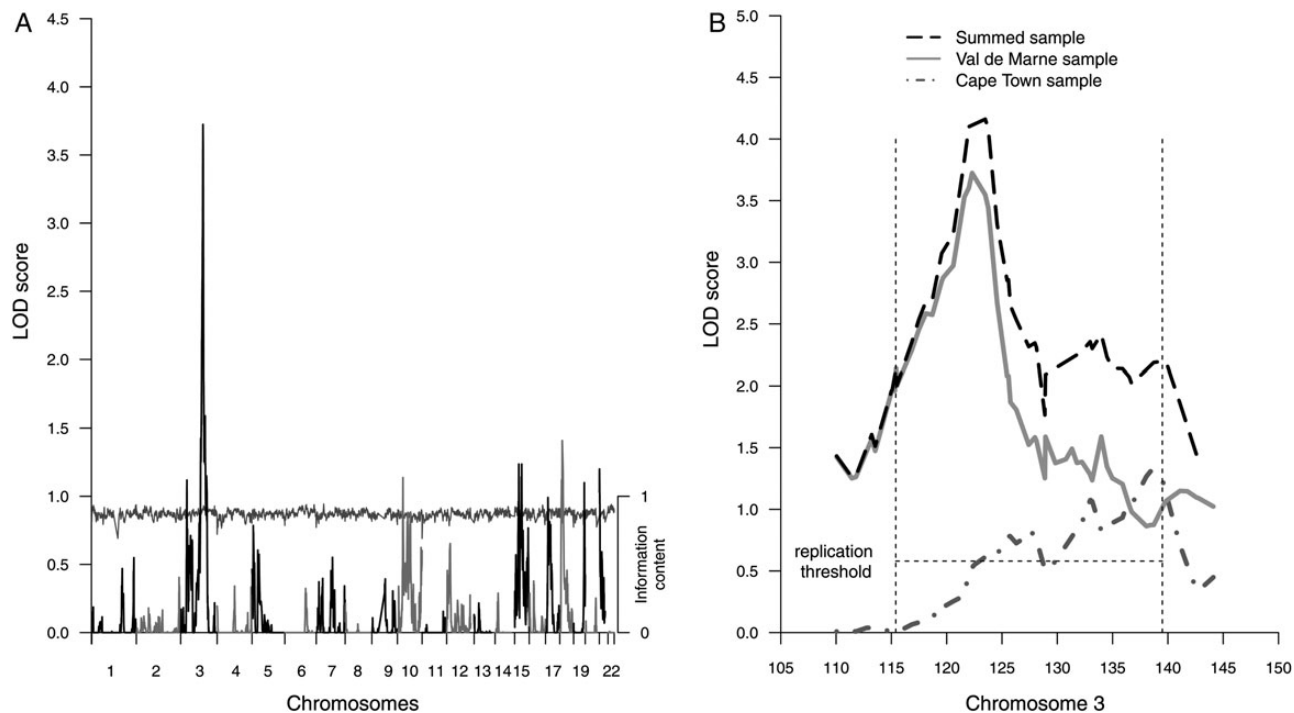


**Figure 2.** Model-free linkage analysis of the IFN $\gamma$ -ESAT<sub>6</sub><sub>BCG</sub> phenotype described in Materials and Methods. *A*, Results for genome-wide analysis for the Val-de-Marne sample, showing multipoint LOD scores (left y-axis) and information content (horizontal line; right y-axis) for the 22 autosomes (x-axis). *B*, Expanded view of the linked chromosome 3 region from 105 to 150 Mb (x-axis). The multipoint LOD score is indicated on the y-axis for the Val-de-Marne sample (solid gray line), the Cape Town sample (double-dashed gray line), and the summed samples (black long-dash line). The horizontal dotted line indicates the significance threshold for replication, and the 2 vertical dotted lines delimit the confidence interval of the linked locus.

of which is associated with mycobacterial infections, including tuberculosis [13]. *ITGB5* encodes the  $\beta$  chain of the integrin heterodimer  $\alpha_v\beta_5$ , which is involved in cell-cell adhesion and has been reported to be essential for the activation of dendritic cells by *M. tuberculosis*-exposed neutrophils [35]. *CD80* and *CD86* encode ligands expressed on antigen-presenting cells that contribute to the regulation of T-cell activation. Mice deficient in both B7.1 (*CD80*) and B7.2 (*CD86*) were found to have enhanced susceptibility to aerosol-mediated infection with *M. tuberculosis* [36], and these 2 molecules have been reported to be equally able to mediate host resistance to *M. tuberculosis* [37]. Furthermore, *CD80* is one of the genes displaying the highest degree of differential expression in primary human dendritic cells after *M. tuberculosis* infection [38].

This linkage result identifies a second major locus in chromosomal region 3q13-22 that controls the amount of IFN- $\gamma$  production in response to ESAT-6, one of the specific antigenic proteins produced by *M. tuberculosis*, when taking into account the IFN- $\gamma$  production, which is shared between the BCG and the ESAT-6 stimulation. We also performed a linkage analysis of the IFN $\gamma$ -ESAT6 phenotype adjusted for IFN $\gamma$ -PPD. The correlation of IFN $\gamma$ -ESAT6 with IFN $\gamma$ -PPD ( $r = 0.61$ ) was stronger than that with IFN $\gamma$ -BCG; PPD contains the ESAT-6 antigen, unlike BCG. Interestingly, the LOD score obtained

for chromosome 3q fell to 2.37 after the adjustment of IFN $\gamma$ -ESAT6 for IFN $\gamma$ -PPD (data not shown). This suggests that the chromosome 3 locus is involved in controlling the IFN- $\gamma$  production more specifically triggered by ESAT-6 stimulation.

## DISCUSSION

We identified 2 significant genome-wide linkage signals corresponding to 2 antimycobacterial immunity phenotypes. The first, on chromosome region 8q12-22, is expected to harbor 1 or several loci that influence IFN- $\gamma$  production triggered by BCG. The second peak, on chromosome region 3q13-22, indicates the location of gene(s) influencing the amount of IFN- $\gamma$  released after ESAT-6 stimulation, following adjustment for the effect common to stimulation with this antigen and with BCG. We were able to replicate the mapping of these loci in a sample from South Africa, using phenotypes that were similar although not identical (IFN- $\gamma$  production in whole blood samples vs PBMCs, measured at 3 days vs 4 days). The 2 populations were also remarkably different in terms of exposure to *M. tuberculosis*. The individuals from South Africa studied live in an area of hyperendemic tuberculosis in which *M. tuberculosis* transmission occurs preferentially in the community [39]. By contrast, tuberculosis endemicity is low in France, and the design of the French study targeted household

tuberculosis contacts. In addition, the 2 cohorts also differed in terms of genetic background. The families in the Val-de-Marne sample belonged to several ethnic groups that we classified into 3 main subpopulations (individuals with a European or North African origin, those with a sub-Saharan African origin, and those with another origin, including Asia), and we found that, within each group, a similar proportion of families contributed to the 2 linkage peaks. By contrast, all individuals from the replication sample studied were from the South African Coloured ethnic group, a population resulting from an admixture of Khoesans (31%), Bantu-speaking Africans (33%), Europeans (16%), and Asians (20%) [40]. The French cohort displayed genetic diversity at the population level, whereas the South African cohort displayed genetic diversity at the individual level. Thus, the replication of linkage findings for these 2 loci in such different settings suggests a robust and, perhaps, universal role of these loci in the control of mycobacteria-triggered IFN- $\gamma$  production in humans.

The IFN $\gamma$ -BCG phenotype corresponds to a general antimycobacterial response. Indeed, IFN- $\gamma$  production in response to BCG stimulation was highly correlated with the response to PPD antigens ( $r = 0.78$ ), and the IFN $\gamma$ -PPD phenotype was also linked to the 8q locus, with a LOD score of 3.03. This suggests that the 8q locus may control a nonspecific component of IFN- $\gamma$  release during mycobacterial infection. The second locus on chromosome 3 corresponds to the IFN $\gamma$ -ESAT6 phenotype analysis when taking into account the IFN- $\gamma$  production which is common between the BCG and the ESAT6 stimulation ( $r = 0.53$ ). This common element may reflect a general capacity for IFN- $\gamma$  production via the T-cell receptor signaling pathway, whereas the IFN $\gamma$ -ESAT6<sub>BCG</sub> phenotype is expected to be more specific to ESAT-6, as this antigen is absent from the BCG strain. ESAT-6 plays an important and specific role in *M. tuberculosis* infection. The adoptive transfer of CD4<sup>+</sup> T cells expressing an ESAT-6-specific T-cell receptor in mice has been reported to lead to strongly enhanced resistance to subsequent airborne *M. tuberculosis* infection [41], indicating the existence of a specific immune response against *M. tuberculosis* infection mediated by the response to ESAT-6. The use of the adjusted IFN $\gamma$ -ESAT6<sub>BCG</sub> phenotype in our analysis strongly increased the linkage peak on chromosome 3q, leading to the mapping of a major locus. We also found that this linkage peak was substantially decreased by adjustment for IFN- $\gamma$  production after stimulation by PPD that contains ESAT-6. Overall, these results are consistent with the view that the chromosome 3q locus plays a role in controlling the IFN- $\gamma$  production more specifically induced by ESAT-6 stimulation.

Not surprisingly, these loci do not overlap with the *TST1* and the *TST2* loci controlling TST positivity per se and the intensity of TST reactivity, respectively [17]. This is consistent with the observed weak correlation between TST and in vitro measurements of *M. tuberculosis* infection (Table 1) and supports the

hypothesis that TST and IFN- $\gamma$  production by PBMCs are markers of different and complementary aspects of antimycobacterial immunity [8]. In particular, the *TST1* locus is thought to reflect T cell-independent resistance to *M. tuberculosis* infection. It is also likely that the functions of skin-homing cells are more diverse than the production of IFN- $\gamma$  alone. For instance, the production of the proinflammatory cytokine tumor necrosis factor  $\alpha$  (TNF $\alpha$ ) is thought to play a major role in the initiation of the TST reaction, a hypothesis supported by the overlap of linkage regions between *TST1* and the *TNF1* locus controlling mycobacterium-driven tumor necrosis factor  $\alpha$  production [18, 42]. In this context, the identification of 2 new loci controlling BCG- and ESAT-6-triggered IFN- $\gamma$  production adds 2 new pieces to the puzzle of how human antimycobacterial immunity is assembled.

### Supplementary Data

Supplementary materials are available at <http://jid.oxfordjournals.org>. Consisting of data provided by the author to benefit the reader, the posted materials are not copyedited and are the sole responsibility of the author, so questions or comments should be addressed to the author.

### Notes

**Acknowledgments.** We thank all members of the community who participated in this study; the Centre National de Génotypage, for conducting the genotyping; Aziz Belkadi, for bioinformatic support; and Emmanuelle Jouanguy, Anne Puel, and Capucine Picard, for helpful discussions.

**Financial support.** This work was supported by the Programme Hospitalier de Recherche Clinique (AOR-04-003); the Legs Poix (Chancellerie des Universités de Paris); the French National Research Agency, under the “Investments for the future” program (grant ANR-10-IAHU-01); the European Research Council (ERC-2010-AdG-268777); the Rockefeller University; the Institut National de la Santé et de la Recherche Médicale; Paris Descartes University; the St. Giles Foundation; the Canadian Institutes of Health Research; the Sequella/Aeras Global Tuberculosis Foundation; and the Government of Canada (Banting postdoctoral fellowship 112932 to A. C.).

**Potential conflicts of interest.** All authors: No reported conflicts. All authors have submitted the ICMJE Form for Disclosure of Potential Conflicts of Interest. Conflicts that the editors consider relevant to the content of the manuscript have been disclosed.

### References

1. WHO. A world free of tuberculosis (TB). <http://www.who.int/tb/en/>. Accessed 17 December 2014.
2. Zumla A, Raviglione M, Hafner R, von Reyn CF. Tuberculosis. *N Engl J Med* **2013**; 368:745–55.
3. O’Garra A, Redford PS, McNab FW, Bloom CI, Wilkinson RJ, Berry MPR. The immune response in tuberculosis. *Annu Rev Immunol* **2013**; 31:475–527.
4. Reichman LB. Tuberculin skin testing. The state of the art. *Chest* **1979**; 76(6 Suppl):764–70.
5. Pai M, Riley LW, Colford JM Jr. Interferon- $\gamma$  assays in the immunodiagnosis of tuberculosis: a systematic review. *Lancet Infect Dis* **2004**; 4:761–76.
6. Mahairas GG, Sabo PJ, Hickey MJ, Singh DC, Stover CK. Molecular analysis of genetic differences between *Mycobacterium bovis* BCG and virulent *M. bovis*. *J Bacteriol* **1996**; 178:1274–82.
7. Andersen P, Munk ME, Pollock JM, Doherty TM. Specific immune-based diagnosis of tuberculosis. *Lancet* **2000**; 356:1099–104.
8. Gallant CJ, Cobat A, Hoal EG, Schurr E. Tuberculin Skin test and in vitro assays provide complementary measures of antimycobacterial immunity in children and adolescents. *Chest* **2010**; 137:1071–7.
9. Salgame P, Geadas C, Collins L, Jones-López E, Ellner JJ. Latent tuberculosis infection—Revisiting and revising concepts. *Tuberc Edinb Scotl* **2015**; 95:373–84.

10. Abel L, El-Baghdadi J, Bousfiha AA, Casanova J-L, Schurr E. Human genetics of tuberculosis: a long and winding road. *Philos Trans R Soc B Biol Sci* **2014**; 369:20130428.
11. Alcaïs A, Fieschi C, Abel L, Casanova J-L. Tuberculosis in children and adults: two distinct genetic diseases. *J Exp Med* **2005**; 202:1617–21.
12. Casanova J-L, Abel L. Genetic dissection of immunity to mycobacteria: the human model. *Annu Rev Immunol* **2002**; 20:581–620.
13. Boisson-Dupuis S, Bustamante J, El-Baghdadi J, et al. Inherited and acquired immunodeficiencies underlying tuberculosis in childhood. *Immunol Rev* **2015**; 264:103–20.
14. Jepson A, Fowler A, Banya W, et al. Genetic regulation of acquired immune responses to antigens of *Mycobacterium tuberculosis*: a study of twins in West Africa. *Infect Immun* **2001**; 69:3989–94.
15. Sepulveda RL, Heiba IM, King A, Gonzalez B, Elston RC, Sorensen RU. Evaluation of tuberculin reactivity in BCG-immunized siblings. *Am J Respir Crit Care Med* **1994**; 149(3 Pt 1):620–4.
16. Stein CM, Zalwango S, Malone LL, et al. Genome scan of *M. tuberculosis* infection and disease in Ugandans. *PLoS One* **2008**; 3:e4094.
17. Cobat A, Gallant CJ, Simkin L, et al. Two loci control tuberculin skin test reactivity in an area hyperendemic for tuberculosis. *J Exp Med* **2009**; 206:2583–91.
18. Cobat A, Poirier C, Hoal E, et al. Tuberculin skin test negativity is under tight genetic control of chromosomal region 11p14–15 in settings with different tuberculosis endemicities. *J Infect Dis* **2015**; 211:317–21.
19. Cobat A, Gallant CJ, Simkin L, et al. High heritability of antimycobacterial immunity in an area of hyperendemicity for tuberculosis disease. *J Infect Dis* **2010**; 201:15–9.
20. Tao L, Zalwango S, Chervenak K, et al. Genetic and shared environmental influences on interferon- $\gamma$  production in response to *Mycobacterium tuberculosis* antigens in a Ugandan population. *Am J Trop Med Hyg* **2013**; 89:169–73.
21. Stein CM, Guwatudde D, Nakakeeto M, et al. Heritability analysis of cytokines as intermediate phenotypes of tuberculosis. *J Infect Dis* **2003**; 187:1679–85.
22. Aissa K, Madhi F, Ronsin N, et al. Evaluation of a model for efficient screening of tuberculosis contact subjects. *Am J Respir Crit Care Med* **2008**; 177:1041–7.
23. den Boon S, van Lill SWP, Borgdorff MW, et al. High prevalence of tuberculosis in previously treated patients, Cape Town, South Africa. *Emerg Infect Dis* **2007**; 13:1189–94.
24. Alcaïs A, Abel L. Maximum-likelihood-binomial method for genetic model-free linkage analysis of quantitative traits in sibships. *Genet Epidemiol* **1999**; 17:102–17.
25. Cobat A, Abel L, Alcaïs A. The maximum-likelihood-binomial method revisited: a robust approach for model-free linkage analysis of quantitative traits in large sibships. *Genet Epidemiol* **2011**; 35:46–56.
26. Lander E, Kruglyak L. Genetic dissection of complex traits: guidelines for interpreting and reporting linkage results. *Nat Genet* **1995**; 11:241–7.
27. Nyholt DR. All LODs are not created equal. *Am J Hum Genet* **2000**; 67:282–8.
28. Price AL, Patterson NJ, Plenge RM, Weinblatt ME, Shadick NA, Reich D. Principal components analysis corrects for stratification in genome-wide association studies. *Nat Genet* **2006**; 38:904–9.
29. Roberts SB, MacLean CJ, Neale MC, Eaves LJ, Kendler KS. Replication of linkage studies of complex traits: an examination of variation in location estimates. *Am J Hum Genet* **1999**; 65:876–84.
30. Puel A, Ziegler SF, Buckley RH, Leonard WJ. Defective IL7R expression in T(-)B(+)NK(+) severe combined immunodeficiency. *Nat Genet* **1998**; 20:394–7.
31. Jacobs SR, Michalek RD, Rathmell JC. IL-7 is essential for homeostatic control of T cell metabolism in vivo. *J Immunol* **2010**; 184:3461–9.
32. Dziarski R, Wang Q, Miyake K, Kirschning CJ, Gupta D, MD-2 enables Toll-like receptor 2 (TLR2)-mediated responses to lipopolysaccharide and enhances TLR2-mediated responses to Gram-positive and Gram-negative bacteria and their cell wall components. *J Immunol* **2001**; 166:1938–44.
33. Baghdadi JE, Orlova M, Alter A, et al. An autosomal dominant major gene confers predisposition to pulmonary tuberculosis in adults. *J Exp Med* **2006**; 203:1679–84.
34. Grant AV, El-Baghdadi J, Sabri A, et al. Age-dependent association between pulmonary tuberculosis and common TOX variants in the 8q12–13 linkage region. *Am J Hum Genet* **2013**; 92:407–14.
35. Hedlund S, Persson A, Vujic A, Che KF, Stendahl O, Larsson M. Dendritic cell activation by sensing *Mycobacterium tuberculosis*-induced apoptotic neutrophils via DC-SIGN. *Hum Immunol* **2010**; 71:535–40.
36. Bhatt K, Uzelac A, Mathur S, McBride A, Potian J, Salgame P. B7 Costimulation Is Critical for Host Control of Chronic *Mycobacterium tuberculosis* Infection. *J Immunol* **2009**; 182:3793–800.
37. Bhatt K, Kim A, Kim A, Mathur S, Salgame P. Equivalent functions for B7.1 and B7.2 costimulation in mediating host resistance to *Mycobacterium tuberculosis*. *Cell Immunol* **2013**; 285:69–75.
38. Barreiro LB, Tailleux L, Pai AA, Gicquel B, Marioni JC, Gilad Y. Deciphering the genetic architecture of variation in the immune response to *Mycobacterium tuberculosis* infection. *Proc Natl Acad Sci U S A* **2012**; 109:1204–9.
39. Verver S, Warren RM, Munch Z, et al. Proportion of tuberculosis transmission that takes place in households in a high-incidence area. *Lancet* **2004**; 363:212–4.
40. Chimusa ER, Daya M, Möller M, et al. Determining ancestry proportions in complex admixture scenarios in South Africa using a novel proxy ancestry selection method. *PLoS One* **2013**; 8:e73971.
41. Gallegos AM, Pamer EG, Glickman MS. Delayed protection by ESAT-6-specific effector CD4+ T cells after airborne *M. tuberculosis* infection. *J Exp Med* **2008**; 205:2359–68.
42. Cobat A, Hoal EG, Gallant CJ, et al. Identification of a major locus, TNF1, that controls BCG-triggered tumor necrosis factor production by leukocytes in an area hyperendemic for tuberculosis. *Clin Infect Dis* **2013**; 57:963–70.